catalysts

MDPI

Article

# Photocatalytic Performance and Degradation Mechanism of Aspirin by $TiO_2$ through Response Surface Methodology

**Lezhuo Li [1], Qiuling Ma [2], Sanfan Wang [1], Sanxiang Song [1], Bo Li [2,3], Ruonan Guo [2], Xiuwen Cheng [2,3,*] and Qingfeng Cheng [4]**

1 Engineering Research Center for Cold and Arid Regions Water Resource Comprehensive Utilization (Ministry of Education), School of Environmental and Municipal Engineering, Lanzhou Jiaotong University, Lanzhou 730070, China; lilezhuo@163.com (L.L.); sfwang1612@163.com (S.W.); ssx156@163.com (S.S.)

2 Key Laboratory of Western China's Environmental Systems (Ministry of Education), College of Earth and Environmental Sciences, Lanzhou University, Lanzhou 730000, China; mql2016@lzu.edu.cn (Q.M.); lb2017@lzu.edu.cn (B.L.); guorn14@lzu.edu.cn (R.G.)

3 Key Laboratory of Comprehensive and Highly Efficient Utilization of Salt Lake Resources, Qinghai Institute of Salt Lakes, Chinese Academy of Sciences, Xinning Road 18, Chengxi District, Xining 810008, China

4 College of Resources and Environment, Chengdu University of Information Technology, Chengdu 610225, China; chqf185@163.com

* Correspondence: chengxw@lzu.edu.cn; Tel.: +86-931-891-1843

Received: 16 January 2018; Accepted: 13 March 2018; Published: 16 March 2018

**Abstract:** In the present work, the photocatalytic performance of P25$TiO_2$ was investigated by means of the degradation of aspirin, while the reaction system was systematically optimized by central composite design (CCD) based on the response surface methodology (RSM). In addition, three variables of initial pH value, initial aspirin concentration and P25 concentration were selected to assess the dependence of degradation efficiencies of aspirin. Meanwhile, a predicted model of degradation efficiency was estimated and checked using analysis of variance (ANOVA). The results indicated that the PC removal of aspirin by P25 was significantly influenced by all these variables in descending order as follows: P25 concentration > initial aspirin concentration > initial pH value. Moreover, the parameters were optimized by the CCD method. Under the conditions of an initial pH value of 5, initial aspirin concentration of 10 mg/L and P25 concentration of 50 mg/L, the degradation efficiency of aspirin was 98.9%with 60 min of Xenon lamp irradiation. Besides, based on the liquid chromatography-mass spectrometry measurements, two main PC degradation pathways of aspirin by $TiO_2$ were deduced and the tentative degradation mechanism was also proposed.

**Keywords:** photocatalysis; aspirin; central composite design; response surface methodology; $TiO_2$

## 1. Introduction

Among the large number of various organic pollutants that may enter into water resources, pharmaceuticals and personal care products (PPCPs) in surface and ground waters have been a major environmental concern [1,2]. Aspirin, known as acetylsalicylic acid (ASA), is commonly used as a classic non-steroidal anti-inflammatory drug (NSAID) to relieve minor aches and treat inflammation and cardiovascular diseases [3,4]. However, this type of pharmaceutical has been detected in the aquatic environment at trace concentrations (ng to μg/L), which can prolong exposure to environmentally relevant concentration and considerably increase the toxicity considerably, resulting in negative consequences for aquatic life and human beings [5–7]. Thus, it is indeed necessary to explore the way to remove these PPCPs, such as aspirin, from aqueous environments.

In recent decades, various wastewater treatments, such as anaerobic processes and activated sludge, have been employed for the degradation of organics, which are not so effective when treating the environment issue of PPCPs [8]. Therefore, researchers have found that advanced oxidation processes (AOPs) can eliminate the refractory contaminants (including emerging contaminants and PPCPs) in aqueous environments, which deserves major attention [9–14]. Moreover, one of these technologies is solar photocatalysis (PC), which can degrade organic pollutants by means of the photocatalytic reaction promoted by the action of light on the surface of a semiconductor acting as a photocatalyst [15]. Among various photocatalysts, $TiO_2$ has been widely studied since Honda pioneered the water splitting of $TiO_2$ photoanodes in 1972 [16], which displays strong chemical stability, non-toxicity, low cost and several unique characteristics. Thus, this has been proven to be a promising technology for the decontamination of these refractory pollutants [17,18]. Li et al. reported the C-N-S-$TiO_2$ electrode that was decorated with Pd exhibited enhanced PC degradation of aspirin [19]. However, during the conventional studies, the optimization of degradation efficiency of aspirin is usually performed using a single variable method, which is time consuming and cost expensive. Furthermore, it is difficult to predict the proper optimum and interactions between different variables [20]. As demonstrated, statistical programs have been invented for carrying out a large number of experiments in a shorter period of time and more efficiently to obtain optimum conditions, which can overcome these aforementioned defects rationally [21,22]. Response surface methodology (RSM), as a statistical method, is used to generate a model, analyze the effects of operating parameters and optimize the process conditions [23]. Furthermore, the central composited design (CCD) is a standard RSM design to analyze the relationship between the several variables and one or more response variables, which can also create a second-order response surface model in the optimization of processes [22,24].

Accordingly, in the present study, the photocatalytic degradation performance and TOC measurement of aspirin by $TiO_2$(P25) under simulated solar irradiation was studied. Additionally, various influencing parameters, such as initial pH value, initial aspirin concentration and P25 concentration, were employed to assess the effect of individual variables and interaction of several variables on PC removal efficiency through the CCD method based on RSM. Besides, PC degradation intermediates and pathways of aspirin by $TiO_2$ were proposed based on the high-performance-liquid chromatography-mass spectrometry/mass spectrometry (HPLC-MS/MS) and ions chromatography (IC) measurements. In addition, the PC degradation mechanism by $TiO_2$ was also deduced.

## 2. Results and Discussion

### *2.1. PC Removal Degradation of Aspirin*

Aspirin, as a common non-steroidal anti-inflammatory (NSAIDs) drug, has been widely used to reduce fever and relieve minor pains and aches. However, this type of pharmaceutical has already been detected in the effluents of sewage and might pose a potential risk to humans. Thus, this was employed to be the target pollutant to evaluate the PC performance of the P25 in this study (Figure 1). Furthermore, the absorbance of the sample in the dark and the photolysis of the aspirin solution were also measured for references. As seen from Figure 1, less than 5% of aspirin could self-decompose when the solution was directly irradiated by the Xenon lamp without the addition of P25, indicating that aspirin was relatively stabilized under Xenon lamp illumination. Besides, when the catalysis existed with the lamp turned off, only 9% of aspirin was removed, which corresponded to the absorbance capacity of the P25 nano-catalyst. We noted that P25 resulted in higher degradation efficiency of aspirin, with68.5% of aspirin removed within 60 min of Xenon lamp illumination. This implied that $TiO_2$ had superior PC performance, which is consistent with other studies [25–27]. In addition, Figure 1 also showed TOC results of aspirin mineralization through PC process. As seen from Figure 1, the high PC mineralization rate of 60.9% was achieved under 60 min of irradiation, implying that P25 had high PC capacity for mineralization of aspirin, which leads to the formation of $CO_2$ and $H_2O$ molecules.

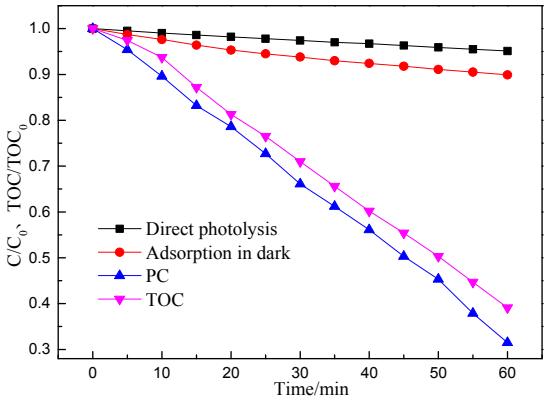


**Figure 1.** Xenon lamp photocatalytic degradation rate and total organic carbon (TOC) result of aspirin over P25 (reaction conditions: the pH value of 7, the aspirin concentration of 20 mg/L and the P25 concentration of 35 mg/L).

### 2.2. Multivariable Experimental Design

Commonly, the PC degradation efficiency of aspirin could be simultaneously influenced by several variables, such as initial aspirin concentration, initial pH and the content of photocatalyst [28,29]. However, it was difficult to find interacting effects among these independent variables from the single-variable optimization experiments, which has been reported by many studies. Hence, the CCD experiment based on the RSM method was aiming to overcome this problem. Following the method shown in Section 3.2, 17 experiments were conducted and the experimental data in CCD for PC degradation efficiency of aspirin are displayed in Table 1. In addition, the experimental conditions for response factor (Y) corresponded to the photocatalytic degradation efficiencies of aspirin (%) after 60 min of irradiation.

**Table 1.** Experimental design matrix and the value of responses based on experiment run.

| Run | Coded Values | | | Independent Variables | | | Degradation Efficiency/% | |
|---|---|---|---|---|---|---|---|---|
| | $X_1$ | $X_2$ | $X_3$ | $X_1$ | $X_2$ | $X_3$ | Experimental | Predicted |
| 1 | −1 | +1 | −1 | 5.00 | 30.00 | 20.00 | 64.2 | 62.0 |
| 2 | 0 | 0 | 0 | 7.00 | 20.00 | 35.00 | 68.4 | 68.2 |
| 3 | 0 | 0 | $-\alpha$ | 7.00 | 20.00 | 9.77 | 70.1 | 66.2 |
| 4 | 0 | $+\alpha$ | 0 | 7.00 | 36.82 | 35.00 | 57.6 | 63.9 |
| 5 | 0 | 0 | $+\alpha$ | 7.00 | 20.00 | 60.23 | 84.5 | 93.5 |
| 6 | +1 | −1 | +1 | 9.00 | 10.00 | 50.00 | 81.9 | 80.2 |
| 7 | −1 | +1 | +1 | 5.00 | 30.00 | 50.00 | 89.9 | 81.0 |
| 8 | $-\alpha$ | 0 | 0 | 3.64 | 20.00 | 35.00 | 67.2 | 75.0 |
| 9 | −1 | −1 | +1 | 5.00 | 10.00 | 50.00 | 98.9 | 94.1 |
| 10 | −1 | −1 | −1 | 5.00 | 10.00 | 20.00 | 78.6 | 78.3 |
| 11 | $+\alpha$ | 0 | 0 | 10.36 | 20.00 | 35.00 | 60.1 | 57.9 |
| 12 | +1 | +1 | +1 | 9.00 | 30.00 | 50.00 | 76.3 | 72.7 |
| 13 | +1 | +1 | −1 | 9.00 | 30.00 | 20.00 | 54.7 | 55.6 |
| 14 | +1 | −1 | −1 | 9.00 | 10.00 | 20.00 | 61.2 | 66.2 |
| 15 | 0 | 0 | 0 | 7.00 | 20.00 | 35.00 | 68.5 | 68.2 |
| 16 | 0 | 0 | 0 | 7.00 | 20.00 | 35.00 | 68.7 | 68.2 |
| 17 | 0 | $-\alpha$ | 0 | 7.00 | 3.18 | 35.00 | 84.6 | 83.8 |

Generally, according to the experimental dates, a semi-empirical second-order polynomial equation consisting of 10 statistically significant coefficients was estimated by computer simulation programming, which applied the least square method using Design-Expert 8.0 as follows:

$$Y = 68.22 - 5.08X_1 - 5.92X_2 + 8.24X_3 + 1.41X_1X_2 - 0.46X_2X_3 + 0.79X_1X_3 - 0.64{X_1}^2 + 2.00{X_2}^2 + 4.19{X_3}^2 \quad (1)$$

where Y was the predicted response; and $X_1$, $X_2$ and $X_3$ corresponded to initial pH value, initial aspirin concentration and P25 concentration, respectively. Besides, the coefficients in the polynomial equation, which included linear coefficients, cross product coefficients and quadratic coefficients, represented the weight of variables and the interaction between them [30]. As calculated from the model of Equation (1), the predicted values for degradation of aspirin by P25 are also listed in Table 1. Meanwhile, the correction between experimental values of degradation rate of aspirin and the predicted values are analyzed and shown in Figure 2. Noticeably, a high correlation coefficient ($R^2$) of 0.8506 was obtained, which indicates consistency between experimental and predicted values and suggests that the model had a good linear fitting and explained the studied experimental range very well.

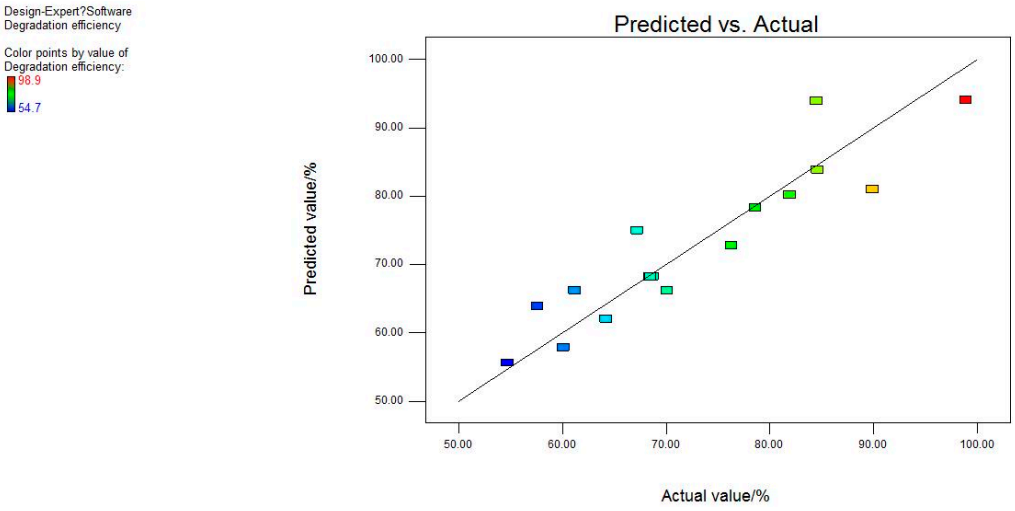


**Figure 2.** Correction between predicted and experimental photocatalytic (PC) degradation efficiencies of aspirin by P25.

Furthermore, the model was checked using the analysis of variance (ANOVA), which could also analyze the statistical significance and effects of regression coefficients. In the CCD study, A *p*-value (significant probability value) lower than 0.05 indicated that the model terms were significant, while values greater than 0.1 indicates no significance [31]. As seen from Table 2, the variables of initial pH value ($X_1$), initial aspirin concentration ($X_2$) and P25 concentration ($X_3$) were all highly significant as the p-values were all below 0.05. Thus, the response factor (degradation rate of aspirin) were indeed influenced by these three variables. In addition, the F-value was used to check the statistical significance with a higher value representing a larger influence [31]. This suggested that the significance of variables fitted the following order: $X_3 > X_2 > X_1$, which is consistent with the weight of variables shown in the predicted model (Equation (1)). Furthermore, the ANOVA results also displayed that the predicted model ($p$-value < 0.05) was reliable for simulating and optimizing the PC decomposition of aspirin by P25.

**Table 2.** Analysis of variance (ANOVA) for the derived response surface methodology (RSM) model.

| Source | Sum of Squares | Degree of Freedom | Mean Square | F-value | *p*-value |
|---|---|---|---|---|---|
| Model | 2041.50 | 9 | 226.83 | 4.43 | 0.0313 |
| $X_1$ | 353.08 | 1 | 353.08 | 6.90 | 0.0341 |
| $X_2$ | 479.33 | 1 | 479.33 | 9.36 | 0.0183 |
| $X_3$ | 927.03 | 1 | 927.03 | 18.10 | 0.0038 |
| $X_1$ $X_2$ | 15.96 | 1 | 15.96 | 0.31 | 0.5940 |
| $X_2$ $X_3$ | 1.71 | 1 | 1.71 | 0.033 | 0.8601 |
| $X_1$ $X_3$ | 4.96 | 1 | 4.96 | 0.097 | 0.7647 |
| $X_1^2$ | 4.60 | 1 | 4.60 | 0.090 | 0.7730 |
| $X_2^2$ | 44.87 | 1 | 44.87 | 0.88 | 0.3804 |
| $X_3^2$ | 197.64 | 1 | 197.64 | 3.86 | 0.0902 |
| Residual | 358.44 | 7 | 51.21 | | |
| Lack of fit | 358.39 | 5 | 71.68 | 3071.92 | 0.0003 |
| Pure error | 0.047 | 2 | 0.023 | | |
| Cor total | 2399.94 | 16 | | | |

R-squared = 0.8506; Adj R-squared = 0.6586.

Therefore, the graphical representations of the regression equation and the information on the primary impact of three factors were evaluated by the 3D response surface plots and the two-dimension contours, which are shown in Figure 3. For aspirin removal, Figure 3a,b showed the combined effect of initial pH value and initial aspirin concentration with the constant concentration of P25 (50 mg/L). When P25 dosage was at a suitable concentration, the degradation rate increased with a decrease in initial pH as well as aspirin concentration. The most efficient removal rate was achieved at the initial aspirin concentration of 10 mg/L with a pH value of 5. As seen from Figure 3c,d, two graphs were developed for the aspirin removal efficiency with varying initial pH value and P25 concentration at a fixed initial aspirin concentration of 10 mg/L. It was clearly seen that the higher PC degradation rate of aspirin was obtained when the P25 concentration reached a maximum of 50 mg/L at a relatively lower pH value of 5, which was consistent with the former result. Subsequently, the relationship between the initial aspirin and P25 concentration affecting the degradation rate was carried out with the initial pH value fixed at 5 and displayed in Figure 3e,f. When the P25 concentration increased from 20 mg/L to 50 mg/L, the PC removal rate of aspirin rose sharply, indicating that P25 concentration had a huge influence on PC activity. Furthermore, the initial aspirin concentration also has an effect, with an optimized dosage of 10 mg/L for the maximum degradation efficiency.

Hence, the experiment in optimum process conditions through RSM based on CCD for the highest desirability was carried out, with the results shown in Figure 4. Obviously, the experimental degradation efficiency of aspirin was 98.9% at the optimized conditions of an initial pH value of 5, initial aspirin concentration of 10 mg/L and P25 concentration of 50 mg/L, respectively. In addition, the software optimized degradation efficiency was 94.1%, which was much closer to the experimental value. This suggests that the predicted model was able to optimize the parameters for PC degradation of aspirin by P25, which was consistent with ANOVA results.

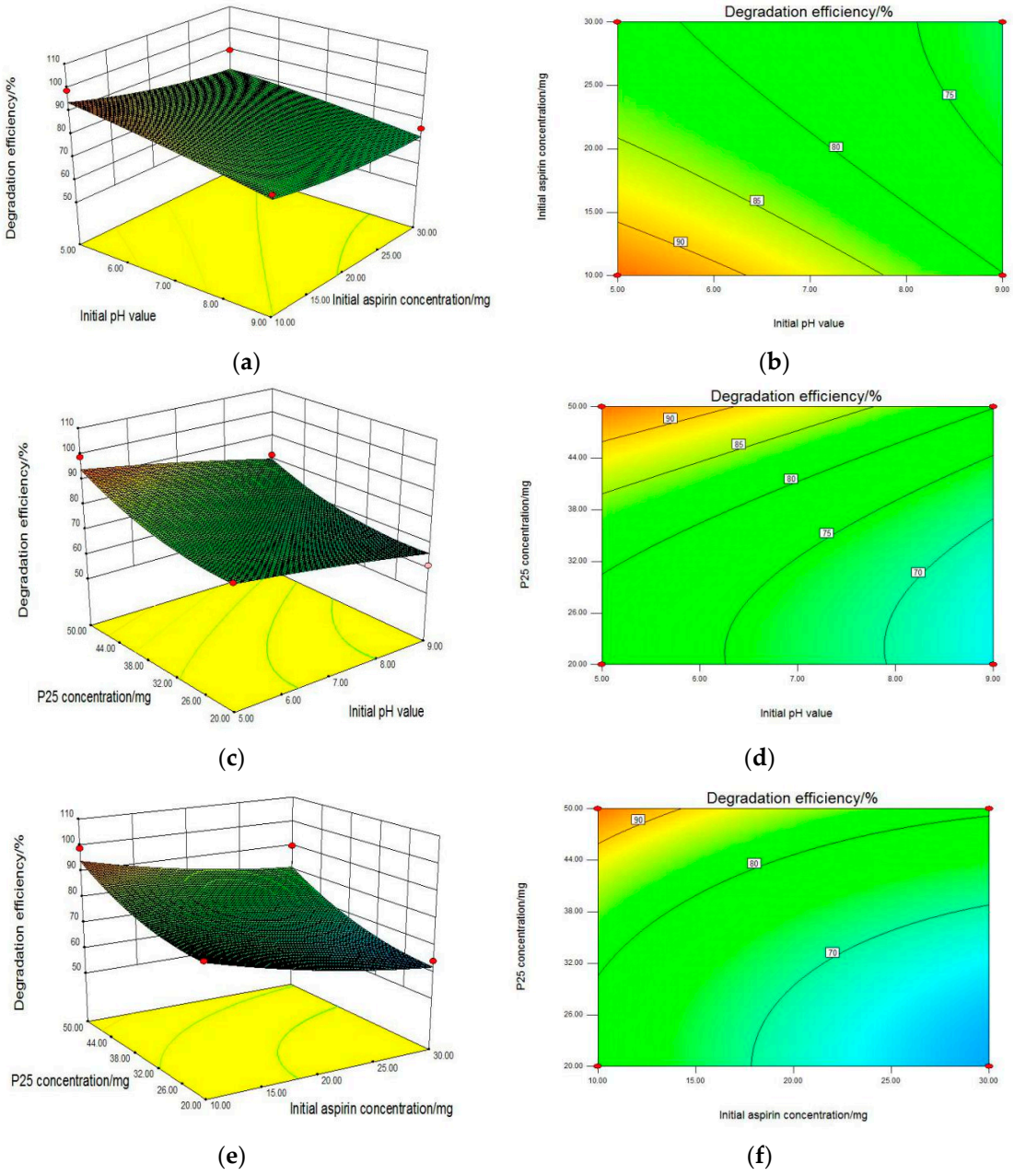


**Figure 3.** 3D response surface plots (**a**,**c**,**e**) and two-dimension contour plots (**b**,**d**,**f**) of interaction between initial pH value ($X_1$), initial aspirin concentration ($X_2$) and P25 concentration ($X_3$) for PC degradation of aspirin by P25, where effect of initial pH value and initial aspirin concentration (**a**,**b**); effect of initial pH value and P25 concentration (**c**,**d**); effect of initial aspirin concentration and P25 concentration (**e**,**f**).

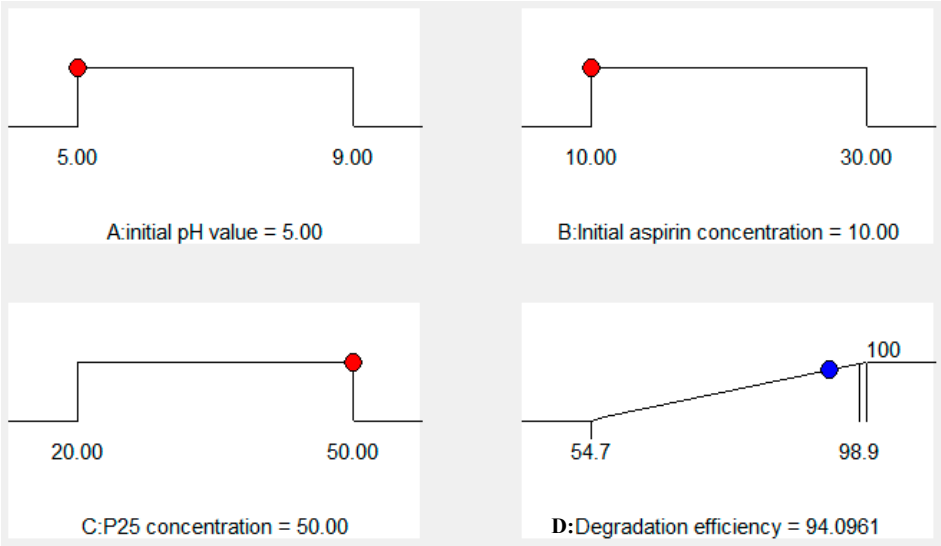


**Figure 4.** Desirability ramp for numerical optimization of independent variables, initial pH value ($X_1$), initial aspirin concentration ($X_2$) and P25 concentration ($X_3$) for the PC degradation efficiency of aspirin by P25. A: initial pH value; B: initial aspirin concentration; C: P25 concentration; D: degradation efficiency

### 2.3. Analysis of Degradation Intermediates

As demonstrated already, the advanced oxidization process (AOP) was widely used in wastewater treatment of pharmaceutical and personal care products (PPCPs) due to being highly active and non-selective between OH radicals and target pollutants [32,33]. However, it might cause the aggregation of the toxicity and recalcitrance of parent compounds, which can cause harm to environment and human nature [34]. Thus, HPLC-MS/MS measurements were carried out to elucidate the intermediates and mechanism of PC decomposition of aspirin by P25 [34]. As displayed in Figure S1, LC-ESI/MS chromatography showed that aspirin was degraded by P25 nano-catalyst within 60 min of Xenon lamp illumination. Thus, we can conclude that several intermediates were formed. The LC-MS/MS spectra of corresponding LC-MS is displayed in Figure 5. Additionally, the structural assignments of all detected intermediates were studied, which are shown in Table 3. Noticeably, the degradation intermediates were detected by comparison with the target pollutant (aspirin, $m/z$ 179) during the PC process, indicating the decomposition and mineralization of aspirin molecules. This is consistent with the TOC results. Therefore, according to the HPLC-MS/MS analyses, nine possible intermediates were identified and figured out, which was in accordance with the previous studies [35] and are listed in Table 3. Furthermore, the PC removal degradation diagram containing two main pathways for elimination of aspirin were proposed, which are plotted in Figure 6.

Compared with the aspirin solution ($m/z$, 179), there was an intermediate with $m/z$ of 135 found, which might be ascribed to the decarboxylation (-$CO_2$) that forms the compound of phenyl acetate (Figure 6, pathway 1). Subsequently, the compound holding $[M+H]^+$ 93 was also detected, which was probably formed through the deacetylation (-$COCH_3$) that reveals the formation of phenol. Furthermore, the addition of 16 mass units of phenol ($m/z$ 93) could be assigned to the hydroxylation, resulting in two intermediates of *o*-dihydroxybenzene and *p*-dihydroxybenzene ($m/z$ 109). Besides, we found that the intermediates with $m/z$ values of 107 and 115 corresponded to the benzoquinone and butenedioic acid, respectively. In addition, the parent compound would be directly oxidized by the photogenerated holes ($h^+$), which consequently leads to the deacetylation (-$COCH_3$) of aspirin. Therefore, this creates the formation of salicylic acid ($m/z$ of 137), which was considered as the other degradation pathway (shown in Figure 6). Furthermore, the product ($m/z$ 153) revealing the addition of 16 mass units compared with salicylic acid was detected, which was probably due to the addition of

hydroxyl radicals (-OH) to form monohydroxylated intermediates. Finally, all the intermediates could be decomposed into small molecules, such as $CO_2$ and $H_2O$, during the PC process.

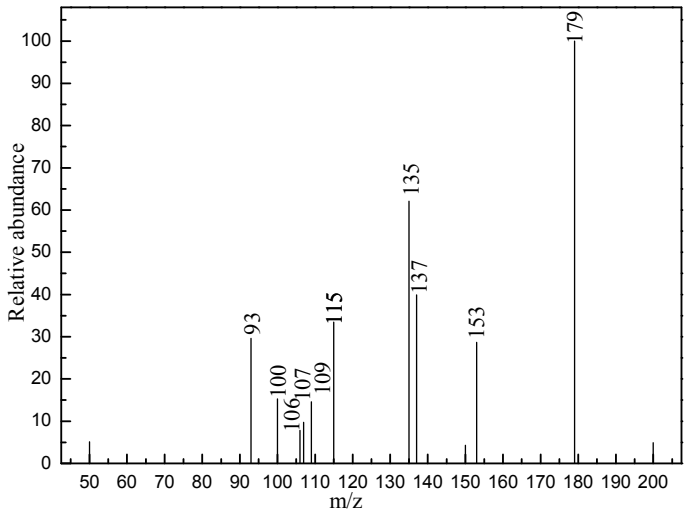


**Figure 5.** Liquid chromatography-mass spectrometry (LC-MS) spectra of main degradation intermediates of aspirin by 60 min of Xenon illumination.

**Table 3.** Possible intermediates of aspirin.

| Number | *m*/*z* | Formula | Possible Structure |
|---|---|---|---|
| Aspirin | 179 | $C_9H_8O_4$ | 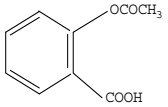 |
| 1 | 135 | $C_8H_8O_2$ | 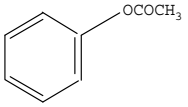 |
| 2 | 115 | $C_4H_4O_4$ | 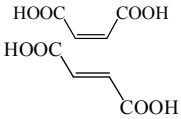 |
| 3 | 109 | $C_6H_6O_2$ | 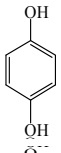 |
| 4 | 107 | $C_6H_4O_2$ | 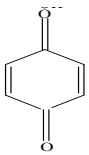 |
| 5 | 93 | $C_6H_6O$ | 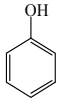 |
| 6 | 137 | $C_7H_6O_3$ | 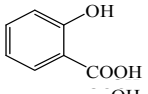 |
| 7 | 153 | $C_7H_6O_4$ | 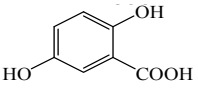 |

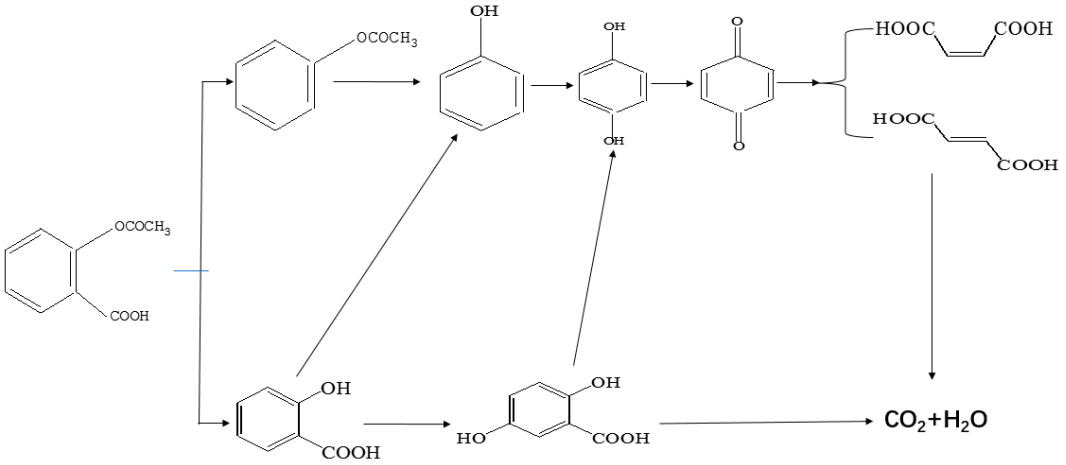


**Figure 6.** Diagram process for PC degradation of aspirin solution by P25.

Thus, as seen from Figure 6, the side chain of aspirin could be altered via decarboxylation (-$CO_2$) of the compound, forming phenyl acetate ($m/z$ of 135) in pathway 1. Therefore, the break in the C-O bond of phenyl acetate yielded phenol ($m/z$ of 93), which subsequently could be attacked by hydroxyl radicals (·OH) on the benzene of ortho-position and para-position. This leads to the formation of *p*-dihydroxybenzene ($m/z$ of 109). Besides, these products might be converted to 1,4-benzoquinone ($m/z$ of 107) due to the self-electron transfer in the molecules. Moreover, we deduced that the benzene ring of benzoquinone was cleaved during the PC process and therefore, yielded butenedioic acid ($m/z$ of 115). Ultimately, all these intermediates could be decomposed to acetic, oxalic acid and formic acid. With prolonged reaction time, these could be mineralized to $CO_2$ and $H_2O$. Besides, the hydroxyl radicals (·OH) played a key role during the whole PC reaction. In pathway 2, the hydroxyl radicals (·OH) could attack the C=O double bonds of aspirin through demethylation (-$CH_3$) to form salicylic acid ($m/z$ 137) and thus, would also attacked the aromatic hydrocarbons by the electrophilic addition on the C=C double bonds of aromatic ring to yield OH-adduct [35,36]. Finally, all the intermediates were completely converted to $CO_2$ and $H_2O$ under the Xenon lamp irradiation, which was highly consistent with the TOC results. Furthermore, we measured the contribution of each species to the PC degradation of aspirin, with the results illustrated in Figure S2. The PC efficiency was 68.5% after 60 min of Xenon lamp irradiation in the absence of any scavenger. When ammonium oxalate (AO) was added into the PC system [37], 49.7% of aspirin could be removed, revealing that $H^+$ could participate in the PC reaction. When tert-butyl alcohol (TBA) was added into the PC reaction system [38], the PC efficiency (5.4%) of aspirin sharply decreased. Additionally, 19.4% of PC efficiency for degradation of aspirin was obtained, suggesting $H_2O_2$ was involved in the aspirin degradation [39]. Similarly, BQ exhibited considerable inhibition of the PC degradation of aspirin (16.3%) [40]. Moreover, with the addition of $K_2Cr_2O_7$ during the PC process [41], the PC efficiency of aspirin (13.1%) was partially suppressed, suggesting that the role of electron ($e^-$) was smaller than that of $H_2O_2$ in our PC system. These results also demonstrated that aspirin would occur several processes, which were finally converted to $CO_2$ and $H_2O$ molecules.

### *2.4. Preliminary Reaction Mechanism*

Figure 7 displayed the proposed PC mechanism of degradation pollutant by P25. As seen, $TiO_2$ with the valence band (VB) maximum potential of 2.91 eV and the conduction band (CB) maximum potential of −029 eV was easily excited to generate holes and electron pairs ($h^+/e^-$) when turning on the light source [25,42]. Thus, under continuous light irradiation, the electrons were excited from the VB to CB, inducing the formation of the photogenerated $H^+$ in the VB. Subsequently, the residual $H^+$ reacted with $H_2O$ in the solution to yield OH radicals, which participated in the degradation of

pollutants due to their highly oxidability. In addition, the separated $e^-$ were then trapped by $O_2$ to produce $O_2^-$ radicals, which were then transferred to OH radicals to initiate the degradation process of organics.

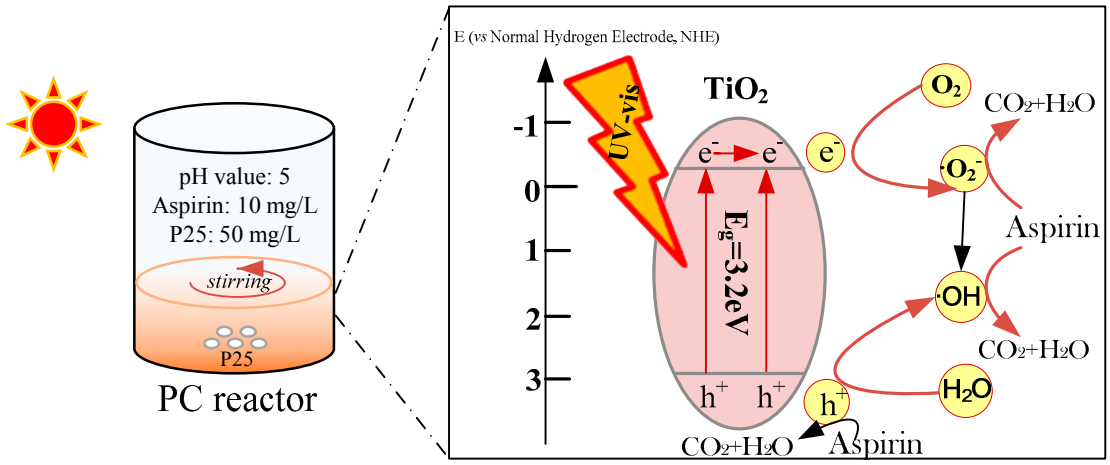


**Figure 7.** Schematic diagram of photocatalytic mechanism of P25.

## 3. Materials and Method

### *3.1. Materials*

Aspirin employed as the target pollutant in the spiked sample was kindly purchased from Sigma-Aldrich without any purification. Titanium dioxide (P25 $TiO_2$) was purchased from Germany Degussa, which was used for photocatalysis before experiments. Besides, methanol and acetic acid were of HPLC grade, while other reagents were all of analytical grade. MilliQ-water was used throughout this experiment.

### *3.2. Design of Experiment*

A CCD based on the RSM of the chemometric approach was used to distinguish the optimum condition for the degradation of aspirin. Analysis of this experimental data was supported by the Design-Expert software (trail version 8, Stat-Ease, Inc., Minneapolis, MN, USA).

In the CCD experimental design, three independent variables of initial pH value, initial aspirin concentration and P25 content on the PC removal efficiency of aspirin were analyzed for their responses. Besides, the rotatable experimental plan consisted of 17 experiments, which was determined by the expression as follows:

$$N = 2^n + 2n + C_0 \quad (2)$$

where N was the total number of experiments required; $n$ was the number of variables with $2n$ being axial runs; and $C_0$ was the center point runs (always chosen between 2 to 5), which was selected as 3 in this experiment. In addition, the three variables were converted to dimensionless ones of $X_1$, $X_2$ and $X_3$ and the coded values at levels of $-1$ and $+1$ corresponded to the low and high levels, respectively. It should be noted that when there were 3 variables, $\alpha$ could be chosen as 1.682 [43]. Furthermore, after several pre-experiments were conducted, the determined values of the selected variables are presented in Table 4.

**Table 4.** Experimental ranges and levels of the variables tested in the central composite design (CCD).

| Independent Variables | Symbol | Actual Values of the Coded Variable Levels | | | | |
|---|---|---|---|---|---|---|
| | | $-1.682(-\alpha)$ | $-1$ | 0 | +1 | $1.682(+\alpha)$ |
| Initial pH | $X_1$ | 3.636 | 5 | 7 | 9 | 10.364 |
| $[Aspirin]_0$ | $X_2$ | 3.18 | 10 | 20 | 30 | 36.82 |
| [P25] | $X_3$ | 9.77 | 20 | 35 | 50 | 60.23 |

### *3.3. PC Degradation Experiments*

Experiments on PC decomposition of aspirin were carried out in a self-made cylindrical quartz reactor to evaluate the PC performance of P25. Typically, the simulated solar light was generated by a 35-W Xenon lamp irradiation (Figure S3). Besides, a radiation mater was used to adjust the luminous intensity of the Xenon lamp, which was controlled to 6.7 $mW \cdot cm^{-3}$. In each run, 100 mL of an aspirin solution (10 mg/L) with a certain amount of P25 sample was added into the reactor, where a special glass atmolyzer was fixed at the bottom of it to maintain the constant air-equilibrated conditions. In order to obtain the adsorption−desorption equilibrium, the reactant mixture was kept in the dark for 30 min before irradiation. Subsequently, the PC activity was started when the Xenon lamp was turned on. At given time intervals, a certain amount of the solution was taken from the reactor and filtrated through a 0.22-μm membrance, which was measured at 35 °C using high performance liquid chromatography (HPLC, Shimadzu LC 10A, Shimadzu company, Kyoto, Japan) system. This system was equipped with a C18 column (150 mm × 20 mm × 4.6 mm i.d., Kromasil KR100-5, Shimadzu company, Tyoto, Japan). The mobile phase was a mixture of 35% methanol and 65% MilliQ-water, which contained 1% acetic acid, and the flow rate was maintained at 1 $mL \cdot min^{-1}$. Furthermore, the sample with the injection volume of 20 μL was detected at the wavelength of 276 nm. Prior to the experiment, the mobile phase should be sonicated for 5 min to remove dissolved gas.

In addition, HPLC coupled with a thermos-LTQ Orbitrap Discovery mass spectrometer was employed in this experiment for detecting the PC degradation intermediates of aspirin. Besides, the measurement used ESI+/ESI− ionization and operated in full-scan mode between 50 and 400 uma. Separation was conducted using a C18 column (150 mm × 20 mm × 4.6 mm i.d., Kromasil KR100-5) with a flow rate of 0.3 $mL \cdot min^{-1}$. It should be noted that the other conditions were in accordance with the HPLC measurements. Furthermore, total organic carbon (TOC) was measured to clarify the mineralization of aspirin using a TOC analyzer (Shimadzu, 5000, Kyoto City, Japan). Besides, several scavenging experiments were conducted to distinguish the contribution of each reactive species. It should be noted that prior to illumination, a scavenger (10 mM) was added into the system. After this, the light was turned on. At given time intervals, the collected sample was filtrated through a 0.22-μm membrane and measured by the HPLC method as mentioned above.

## 4. Conclusions

To conclude, the PC performance and degradation mechanism of aspirin by $TiO_2$ was evaluated and optimized by RSM based on CCD methods. In the present study, 68.5% of the aspirin could be removed within 60 min of Xenon lamp illumination by P25 and the process was further investigated by a decrease in TOC concentration. Besides, according to the RSM results, the variables of initial pH value ($X_1$), initial aspirin concentration ($X_2$) and P25 concentration ($X_3$) could significantly affect the PC degradation performance of aspirin and the significance of which followed the order of $X_3 > X_2 > X_1$. In addition, the CCD method was employed as a powerful tool to optimize these parameters, suggesting that under the optimized conditions of initial pH value of 5, initial aspirin concentration of 10 mg/L and P25 concentration of 50 mg/L, an experimental degradation efficiency of 98.9% could be obtained. This is much closer to the predicted value calculated by the predicted model. Moreover, the tentative mechanism for PC decomposition of aspirin was deduced from HPLC-MS/MS measurements, where two main degradation pathways were proposed. Thus, this study provided the

interacting effects among variables and the mechanism for PC degradation activity of aspirin by $TiO_2$, which opened a gateway for further researches into wastewater treatment.

**Supplementary Materials:** The following are available online at http://www.mdpi.com/2073-4344/8/3/118/s1, Figure S1: Typical LC-ESI/MS chromatography of aspirin degraded by P25 $TiO_2$ nano-catalyst after 60 min Xenon lamp illumination, Figure S2: Effect of each reaction species on PC degradation of aspirin solution by P25, Figure S3: Emission spectrum of 35 W Xenon lamp.

**Acknowledgments:** This work was kindly supported by National Natural Science Foundation of China (51508254), Open fund by Jiangsu Engineering Technology Research Center of Environmental Cleaning Materials (KFK1502), A Project Funded by the Priority Academic Program Development of Jiangsu Higher Education Institutions (PAPD) and Key Laboratory of Comprehensive and Highly Efficient Utilization of Salt Lake Resources, Qinghai Institute of Salt Lakes, Chinese Academy of Sciences.

**Author Contributions:** Xiuwen Cheng and Sanfan Wang designed this study. Lezhuo Li, Qiuling Ma, Sanxiang Song and Qingfeng Cheng wrote the paper. Ruonan Guo and Bo Li performed the photocatalytic performance of P25. Xiuwen Cheng, Sanfan Wang and Sanxiang Song supervised the study. All authors made substantial contributions to the discussion of data and approved the final manuscript.

**Conflicts of Interest:** The authors declare no conflict of interest.

## References

1. Boyd, G.R.; Reemtsma, H.; Grimm, D.A.; Mitra, S. Pharmaceuticals and personal care products PPCPs in surface and treated waters of Louisiana, USA and Ontario, Canada. *Sci. Total Environ.* **2003**, *311*, 135–149. [CrossRef]
2. Gunnarsdottir, R.; Jenssen, P.D.; Jensen, P.E.; Villumsen, A.; Kallenborn, R. A review of wastewater handling in the Arctic with special reference to pharmaceuticals and personal care products PPCPs and microbial pollution. *Ecol. Eng.* **2013**, *50*, 76–85. [CrossRef]
3. Ma, N.; Liu, X.W.; Yang, Y.J.; Li, J.Y.; Mohamed, I.; Liu, G.R.; Zhang, J.Y. Preventive Effect of Aspirin Eugenol Ester on Thrombosis in κ-Carrageenan-Induced Rat Tail Thrombosis Model. *PLoS ONE* **2015**, *10*, 0133125. [CrossRef] [PubMed]
4. Adebayo, G.I.; Williams, J.; Healy, S. Aspirin esterase activity—Evidence for skewed distribution in healthy volunteers. *Eur. J. Int. Med.* **2007**, *18*, 299–303. [CrossRef] [PubMed]
5. Galus, M. Chronic Exposure to Environmentally Relevant Pharmaceutical Concentrations Effects Reproductive and Developmental Physiology in Zebrafsih Danio Rerio. 2014. Available online: https://macsphere.mcmaster.ca/handle/11375/16282 (accessed on 19 February 2018).
6. Agunbiade, F.O.; Moodley, B. Occurrence and distribution pattern of acidic pharmaceuticals in surface water, wastewater, and sediment of the Msunduzi River, Kwazulu-Natal, South Africa. *Environ. Toxicol. Chem.* **2016**, *35*, 36–46. [CrossRef] [PubMed]
7. Vieno, N.M.; Härkki, H.; Tuhkanen, T.; Kronberg, L. Occurrence of pharmaceuticals in river water and their elimination in a pilot-scale drinking water treatment plant. *Environ. Sci. Technol.* **2007**, *41*, 5077–5084. [CrossRef] [PubMed]
8. Bouju, H.; Nastold, P.; Beck, B.; Hollender, J.; Corvini, P.F.; Wintgens, T. Elucidation of biotransformation of diclofenac and 4'hydroxydiclofenac during biological wastewater treatment. *J. Hazard. Mater.* **2016**, *301*, 443–452. [CrossRef] [PubMed]
9. Yu, H.; Nie, E.; Xu, J.; Yan, S.; Cooper, W.J.; Song, W. Degradation of Diclofenac by Advanced Oxidation and Reduction Processes: Kinetic Studies, Degradation Pathways and Toxicity Assessments. *Water Res.* **2013**, *47*, 1909–1918. [CrossRef] [PubMed]
10. Li, W.; Zhou, Q.; Tao, H. Removal of Organic Matter from Landfill Leachate by Advanced Oxidation Processes: A Review. *Int. J. Chem. Eng.* **2010**, *2010*, 1–10. [CrossRef]
11. Shen, R.Q.; Andrews, S.A. Demonstration of 20 pharmaceuticals and personal care products PPCPs as nitrosamine precursors during chloramine disinfection. *Water Res.* **2011**, *45*, 944–952. [CrossRef] [PubMed]
12. Eskandarian, M.R.; Choi, H.; Fazli, M.; Rasoulifard, M.H. Effect of UV-LED wavelengths on direct photolytic and $TiO_2$ photocatalytic degradation of emerging contaminants in water. *Chem. Eng. J.* **2016**, *300*, 414–422. [CrossRef]

13. Arlos, M.J.; Hatat-Fraile, M.M.; Liang, R.; Bragg, L.M.; Zhou, N.Y.; Andrews, S.A.; Servos, M.R. Photocatalytic decomposition of organic micropollutants using immobilized $TiO_2$ having different isoelectric points. *Water Res.* **2016**, *101*, 351–361. [CrossRef] [PubMed]
14. Jallouli, N.; Pastrana-Martínez, L.M.; Ribeiro, A.R.; Moreira, N.F.F.; Faria, J.L.; Hentati, O.; Silva, A.M.T.; Ksibi, M. Heterogeneous photocatalytic degradation of ibuprofen in ultrapure water, municipal and pharmaceutical industry wastewaters using a $TiO_2$/UV-LED system. *Chem. Eng. J.* **2018**, *334*, 976–984. [CrossRef]
15. Zhang, H.; Zong, R.; Zhao, J.; Zhu, Y. Dramatic visible photocatalytic degradation performances due to synergetic effect of $TiO_2$ with PANI. *Environ. Sci. Technol.* **2008**, *42*, 3803–3807. [CrossRef] [PubMed]
16. Fujishima, A.; Honda, K. Photolysis-decomposition of water at surface of an irradiated semiconductor. *Nature* **1972**, *238*, 238–245. [CrossRef]
17. Lu, N.; Quan, X.; Li, J.; Chen, S.; Yu, A.H.; Chen, G.H. Fabrication of Boron-Doped $TiO_2$ Nanotube Array Electrode and Investigation of Its Photoelectrochemical Capability. *J. Phys. Chem. C* **2007**, *111*, 11836–11842. [CrossRef]
18. Nie, J.; Mo, Y.; Zheng, B.; Yuan, H.; Xiao, D. Electrochemical fabrication of lanthanum-doped $TiO_2$ nanotube array electrode and investigation of its photoelectrochemical capability. *Electrochim. Acta* **2013**, *90*, 589–596. [CrossRef]
19. Li, D.; Jia, J.; Zheng, T.; Cheng, X.; Yu, X. Construction and characterization of visible light active Pdnano-crystallite decorated and C-N-S-co-doped $TiO_2$ nanosheet array photoelectrode for enhanced photocatalytic degradation of acetylsalicylic acid. *Appl. Catal. B Environ.* **2016**, *188*, 259–271. [CrossRef]
20. Gupta, V.K.; Fakhri, A.; Agarwal, S.; Sadeghi, N. Synthesis of $MnO_2$/Cellulose fiber Nanocomposites for Rapid Adsorption of Insecticide compound and Optimization by Response Surface Methodology. *Int. J. Biol. Macromol.* **2017**, *102*, 840–846. [CrossRef] [PubMed]
21. Arunkumar, T.; Anand, D.A.; Narendrakumar, G. Application of response surface methodology RSM -CCD for the production of laccases using submerged fermentation. *Int. J. Pharm. Biosci.* **2014**, *5*, B429–B438.
22. Kusmiyati, K.; Amin, N.A.S. Application of central composite design CCD and response surface methodology RSM in the catalytic conversion of methane and ethylene into liquid fuel products. *IEEE Int. Conf. Syst. Man Cybern.* **2004**, *5026*, 5025–5030.
23. Liu, J.; Li, L.; Zhou, L.; Li, B.; Xu, Z. Effect of ultrasound treatment conditions on *Saccharomycescerevisiae* by response surface methodology. *Microb. Pathog.* **2017**, *111*, 497–502. [CrossRef] [PubMed]
24. Torgut, G.; Tanyol, M.; Biryan, F.; Pihtili, G.; Demirelli, K. Application of response surface methodology for optimization of Remazol Brilliant Blue R removal onto a novel polymeric adsorbent. *J. Taiwan Inst. Chem. Eng.* **2017**, *80*, 406–414. [CrossRef]
25. Xu, H.; Ouyang, S.X.; Liu, L.Q.; Reunchan, P.; Umezawa, N.; Ye, J.H. Recent advances in $TiO_2$-based photocatalysis. *J. Mater. Chem. A* **2014**, *2*, 12642–12661. [CrossRef]
26. Ishibashi, K.; Fujishima, A.; Watanabe, T.; Hashimoto, K. Detection of active oxidative species in $TiO_2$photocatalysis using the fluorescence technique. *Electrochem. Commun.* **2000**, *2*, 207–210. [CrossRef]
27. Liang, D.Y.; Cui, C.; Hu, H.H.; Wang, Y.P.; Xu, S.; Ying, B.L.; Li, P.G.; Lu, B.Q.; Shen, H.L. One-step hydrothermal synthesis of anatase $TiO_2$/reduced graphene oxide nanocomposites with enhanced photocatalytic activity. *J. Alloys Compd.* **2014**, *582*, 236–240. [CrossRef]
28. Kinsinger, N.M.; Dudchenko, A.; Wong, A.; Kisailus, D. Synergistic effect of pH and phase in a nanocrystallinetitaniaphotocatalyst. *ACS Appl. Mater. Interfaces* **2013**, *5*, 6247–6254. [CrossRef] [PubMed]
29. Mukherjee, D.; Barghi, S.; Ray, A.K. Preparation and Characterization of the $TiO_2$ Immobilized Polymeric Photocatalyst for Degradation of Aspirin under UV and Solar Light. *Processes* **2013**, *2*, 12–23. [CrossRef]
30. Zhang, B.Z.; Cui, J.D.; Zhao, G.X.; Jia, S.R. Modeling and Optimization of Phenylalanine Ammonia Lyase Stabilization in Recombinant Escherichia coli for the Continuous Synthesis of l-Phenylalanine on the Statistical-Based Experimental Designs. *J. Agric. Food Chem.* **2010**, *58*, 2795–2800. [CrossRef] [PubMed]
31. Khamparia, S.; Jaspal, D. Study of decolorisation of binary dye mixture by response surface methodology. *J. Environ. Manag.* **2017**, *201*, 316–326. [CrossRef] [PubMed]
32. Hisaindee, S.; Meetani, M.A.; Rauf, M.A. Application of LC-MS to the analysis of advanced oxidation process AOP degradation of dye products and reaction mechanisms. *Trac Trends Anal. Chem.* **2013**, *49*, 31–44. [CrossRef]

33. Muruganandham, M.; Suri, R.; Jafari, S.; Sillanpää, M.; Lee, G.J.; Wu, J.J.; Swaminathan, M. Recent Developments in Homogeneous Advanced Oxidation Processes for Water and Wastewater Treatment. *Int. J. Photoenergy* **2014**, *2014*. [CrossRef]
34. Augugliaro, V.; Litter, M.; Palmisano, L.; Soria, J. The combination of heterogeneous photocatalysis with chemical and physical operations: A tool for improving the photoprocess performance. *J. Photochem. Photobiol. C Photochem. Rev.* **2006**, *7*, 127–144. [CrossRef]
35. Cui, Y.; Meng, Q.; Deng, X.; Ma, Q.; Zhang, H.; Cheng, X.; Li, X.; Xie, M.; Cheng, Q. Fabrication of platinum nano-crystallites decorated $TiO_2$nano-tube array photoelectrode and its enhanced photoelectrocatlytic performance for degradation of aspirin and mechanism. *J. Ind. Eng. Chem.* **2016**, *43*, 177–184. [CrossRef]
36. Gou, J.; Ma, Q.; Cui, Y.; Deng, X.; Zhang, H.; Cheng, X.; Li, X.; Xie, M.; Cheng, Q.; Liu, H. Visible light photocatalytic removal performance and mechanism of diclofenac degradation by $Ag_3PO_4$ sub-microcrystals through response surface methodology. *J. Ind. Eng. Chem.* **2017**, *49*, 112–121. [CrossRef]
37. Li, W.J.; Li, D.Z.; Zhang, W.J.; Hu, Y.; He, Y.H.; Fu, X.Z. Microwave Synthesis of $Zn_xCd_{1-x}S$ Nanorods and Their Photocatalytic Activity under Visible Light. *J. Phys. Chem. C* **2010**, *114*, 2154–2159. [CrossRef]
38. Lin, Y.M.; Li, D.Z.; Hu, J.H.; Xiao, G.C.; Wang, J.X.; Li, W.J.; Fu, X.Z. Highly efficient photocatalytic degradation of organic pollutants by PANI-modified $TiO_2$ composite. *J. Phys. Chem. C* **2012**, *116*, 5764–5772. [CrossRef]
39. Chen, Y.M.; Lu, A.H.; Li, Y.; Zhang, L.S.; Yip, H.Y.; Zhao, H.J.; An, T.C.; Wong, P.K. Naturally occurring sphalerite as a novel cost-effective photocatalyst for bacterial disinfection under visible light. *Environ. Sci. Technol.* **2011**, *45*, 5689–5695. [CrossRef] [PubMed]
40. Lalhriatpuia, C.; Tiwari, D.; Tiwari, A.; Lee, S.M. Immobilized Nanopillars-$TiO_2$ in the efficient removal of micro-pollutants from aqueous solutions: Physico-chemical studies. *Chem. Eng. J.* **2015**, *281*, 782–792. [CrossRef]
41. Rimoldi, L.; Meroni, D.; Cappelletti, G.; Ardizzone, S. Green and low cost tetracycline degradation processes by nanometric and immobilized $TiO_2$ systems. *Catal. Today* **2017**, *281*, 38–44. [CrossRef]
42. Gao, B.; Li, X.X.; Ma, Y.W.; Cao, Y.; Hu, Z.Y.; Zhang, X.M.; Fu, J.J.; Huo, K.F.; Chu, P.K. $MnO_2$-$TiO_2$/C nanocomposite arrays for high-performance supercapacitor electrodes. *Thin Solid Films* **2015**, *584*, 61–65. [CrossRef]
43. An, T.C.; An, J.B.; Yang, H.; Li, G.Y.; Feng, H.X.; Nie, X.P. Photocatalytic degradation kinetics and mechanism of antivirus drug-lamivudine in $TiO_2$ dispersion. *J. Hazard. Mater.* **2011**, *197*, 229–236. [CrossRef] [PubMed]